

Hydride Reactivity of Ni^{II}–X–Ni^{II} Entities: Mixed-Valent Hydrido Complexes and Reversible Metal Reduction

Henrike Gehring,^[a] Ramona Metzinger,^[a] Christian Herwig,^[a] Julia Intemann,^[b] Sjoerd Harder,^[b] and Christian Limberg^{*[a]}

Abstract: After the lithiation of PYR-H₂ (PYR²⁻ = [[NC(Me)C(H)C(Me)-NC₆H₃(iPr)₂]₂(C₅H₃N)]²⁻), which is the precursor of an expanded β-diketiminato ligand system with two binding pockets, its reaction with [NiBr₂(dme)] led to a dinuclear nickel(II)–bromide complex, [(PYR)Ni(μ-Br)NiBr] (1). The bridging bromide ligand could be selectively exchanged for a thiolate ligand to yield [(PYR)Ni(μ-SEt)NiBr] (3). In an attempt to introduce hydride ligands, both compounds were treated with KHBET₃. This treatment afforded [(PYR)Ni(μ-H)Ni] (2), which is a

mixed valent Ni^I–μ-H–Ni^{II} complex, and [(PYR-H)Ni(μ-SEt)Ni] (4), in which two tricoordinated Ni^I moieties are strongly antiferromagnetically coupled. Compound 4 is the product of an initial salt metathesis, followed by an intramolecular redox process that separates the original hydride ligand into two electrons, which reduce the metal centres, and a proton, which is trapped

by one of the binding pockets, thereby converting it into an olefin ligand on one of the Ni^I centres. The addition of a mild acid to complex 4 leads to the elimination of H₂ and the formation of a Ni^{II}Ni^{II} compound, [(PYR)Ni(μ-SEt)NiOTf] (5), so that the original Ni^{II}(μ-SEt)Ni^{II}X core of compound 3 is restored. All of these compounds were fully characterized, including by X-ray diffraction, and their molecular structures, as well as their formation processes, are discussed.

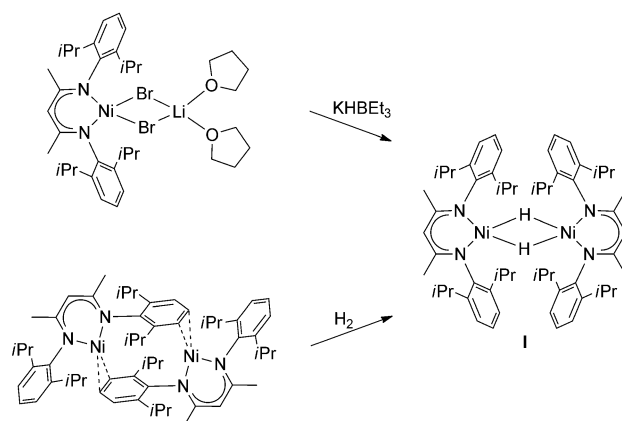
Keywords: bridging ligands • hydrides • mixed-valent compounds • nickel • reduction

Introduction

The combination of nickel and hydride ligands leads to highly reactive systems that are widely utilised in academic and industrial laboratories, such as in the field of homogeneous catalysis for the transformation of organic or inorganic substrates and in the electrolytic generation of H₂.^[1,2] The nickel–hydride functionality also plays a key role in nature. For instance, the central intermediate in the catalytic cycle of [NiFe] hydrogenase is assumed to contain a bridging hydride ligand between the Ni and Fe centres.^[3] Altogether, these factors have led to great interest in investigations on the Ni–H coordination compounds.^[4]

With this background in mind, we are interested in the fundamental hydride/dihydrogen chemistry of dinuclear nickel cores, the results of which may also have some relevance to certain aspects of [NiFe] hydrogenase reactivity

(see below). We used the β-diketiminato ligand system previously because it is known to stabilise both high and low oxidation states^[5] and, furthermore, it can be employed to access complexes with low coordination numbers, which often show interesting reactivities.^[6] In this context, we have recently reported the synthesis of [LNi(μ-H)₂NiL] (I, L = [HC(CMe)NC₆H₃(iPr)₂]⁻; Scheme 1), which was found to be very reactive: On the addition of simple donors (Do), H₂ was immediately reductively eliminated with the concomitant formation of [LNi^I(Do)] complexes.^[7]



Scheme 1. Synthesis of [LNi(μ-H)₂NiL] (I) through two different reaction pathways: A metathesis reaction, starting from a nickel(II) bromide, or oxidative addition of H₂ to a nickel(I) precursor.

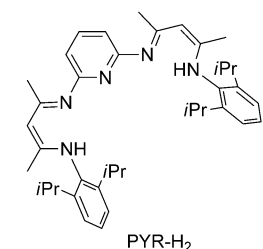
[a] H. Gehring, R. Metzinger, C. Herwig, Prof. Dr. C. Limberg
Institut für Anorganische Chemie
Humboldt-Universität zu Berlin
Brook-Taylor-Strasse 2, 12489 Berlin (Germany)
Fax: (+49) 030-2093-6966
E-mail: christian.limberg@chemie.hu-berlin.de

[b] J. Intemann, Prof. Dr. S. Harder
Stratingh Institute of Chemistry
University of Groningen
Nijenborgh 4, 9747 AG Groningen (Netherlands)

Supporting information for this article is available on the WWW under <http://dx.doi.org/10.1002/chem.201203201>.

Starting from LNi^{I} complexes in the complete absence of suitable donor molecules, the reverse reaction, that is, the oxidative addition of H_2 , has also been observed (Scheme 1).^[8,9] This result is particularly valuable with regard to the mechanistic discussion on H_2 activation at the $[\text{NiFe}]$ hydrogenase active site: Interestingly, a mechanism that is based on the oxidative addition of H_2 to a Ni^{I} intermediate has been derived for these enzymes from theoretical results^[10] and this proposal now has some experimental support. Moreover, it was shown that a nickel(II)–hydride dimer (**I**) can accept one electron to give a mixed-valent $\text{Ni}^{\text{I}}\text{Ni}^{\text{II}}$ –hydride compound, $\text{K}[\text{LNi}(\mu\text{-H})_2\text{NiL}]$, with localised spins.^[11] However, further reduction triggers a complicated reaction sequence that reproducibly—and in good yields—leads to the complex $\text{K}_2[(\text{LNi})_2\text{Ni}(\mu\text{-H})_4]$, which features an unprecedented Ni_3H_4 core.^[11] Altogether, these results showed that β -diketiminato-ligated nickel–hydride moieties can offer versatile redox chemistry, thereby leading to interesting electronic situations and reactivities.

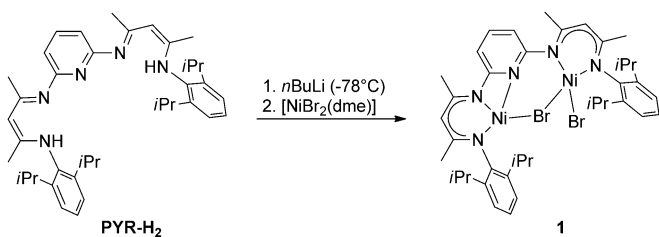
The work described herein builds upon these results. It sets out with a ligand system, $[[\text{NC}(\text{Me})\text{C}(\text{H})\text{C}(\text{Me})\text{NC}_6\text{H}_3\text{-}(\text{iPr})_2]_2(\text{C}_5\text{H}_3\text{N})]^{2-}$ (PYR^{2-}), in which two diketiminato units are prearranged by a pyridine linker for the complexation of two metal centres in a fashion that allows for their cooperation.



Therefore, this ligand system is ideally suited for studies on multimetallic complexes; for example, several zinc, calcium, and magnesium–amidoborane and –hydride complexes, have successfully been accessed by using PYR or related ligands.^[12] Herein, we report the results that were obtained by employing this ligand for the investigation of dinuclear nickel–hydride chemistry.

Results and Discussion

Similar to our earlier investigations (Scheme 1), our first target was the synthesis of a suitable nickel–bromide precursor. Hence, PYR-H_2 was lithiated with $n\text{BuLi}$ and treated with $[\text{NiBr}_2(\text{dme})]$ ($\text{dme} = 1,2\text{-dimethoxyethane}$; Scheme 2) to yield the dinickel(II) complex $[(\text{PYR})\text{Ni}(\mu\text{-Br})\text{NiBr}]$ (**1**)



Scheme 2. Synthesis of $\text{Ni}^{\text{II}}\text{Ni}^{\text{II}}\text{-Br}$ complex **1**.

as a dark-green solid. By cooling a solution in toluene/ n -hexane to -30°C , crystals that were suitable for X-ray diffraction could be obtained.

The molecular structure of complex **1** is shown in Figure 1. One nickel ion is in an almost square-planar coordination environment, whereas the other is surrounded by

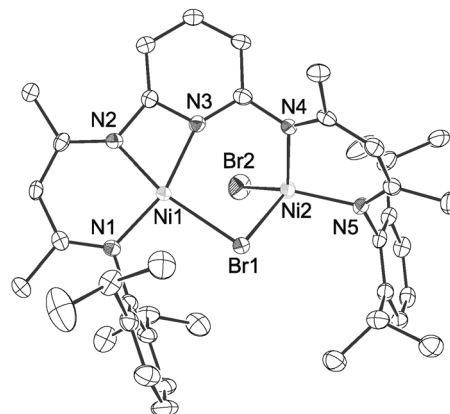


Figure 1. Molecular structure of complex **1**; ellipsoids are set at 50% probability. Hydrogen atoms are omitted for clarity. Selected bond lengths [Å] and angles [°]: Ni1-Ni1 1.884(2), Ni2-Ni1 1.837(3), Ni3-Ni1 1.950(2), Ni1-Br1 2.3568(6), Ni1-Ni2 3.4290(7), Ni2-Br1 2.4455(5), Ni2-Br2 2.3544(6), Ni2-N4 1.944(2), Ni2-N5 1.949(2), Ni2-N3 3.059(8); Ni1-Ni1-N2 93.87(11), Ni1-Ni1-Br1 98.73(8), Br1-Ni1-N3 98.67(7), N3-Ni1-N2 68.72(11), N4-Ni2-N5 94.71(10), Br1-Ni2-Br2 108.42(2), Br2-Ni2-N4 117.81(8), N5-Ni2-Br1 104.43(7).

its ligand in a slightly distorted tetrahedral fashion; there is one bridging bromide ligand between the Ni ions and one additional terminal bromide ligand. The Br1-Ni2-Br2 , Br2-Ni2-N4 , N4-Ni2-N5 , and N5-Ni2-Br1 angles are 108.42(2), 117.81(8), 94.71(10), and 104.43(7)° and, thus, are close to the valence angles for a tetrahedral coordination geometry (109.47°). The Ni2-N4 and Ni2-N5 distances (1.994(2) and 1.949(2) Å) are somewhat longer than Ni1-Ni1 and Ni2-Ni1 (1.884(2) and 1.837(3) Å), but similar to the corresponding distances in related tetrahedrally coordinated nickel complexes that contain β -diketiminato ligands.^[8] In addition, Ni1 has a contact with the N3 atom, at a distance of 1.950(2) Å, although the corresponding pyridyl unit is considerably misaligned; therefore, donation has to proceed through a “bent bond”. Bearing in mind that some complexes are known that feature a bridging pyridyl ligand unit between two metal centres,^[13] in principle, such a binding mode could be relevant here, too. However, considering that the distance between the Ni2 and N3 atoms is 3.059(8) Å, this effect doesn't seem to apply.

The magnetic moment for compound **1** in solution at room temperature ($\mu_{\text{eff}} = 3.03 \mu_{\text{B}}$), as determined by using the Evans method, is in accordance with the spin only (s.o.) value for two unpaired electrons on one nickel centre with a total spin quantum number of $S = 1$ ($\mu_{\text{s.o.}} = 2.83 \mu_{\text{B}}$). Because the average magnetic moment for tetrahedral nickel(II) complexes is $\mu = (3.20 \pm 0.20)$,^[14] it is reasonable to assume

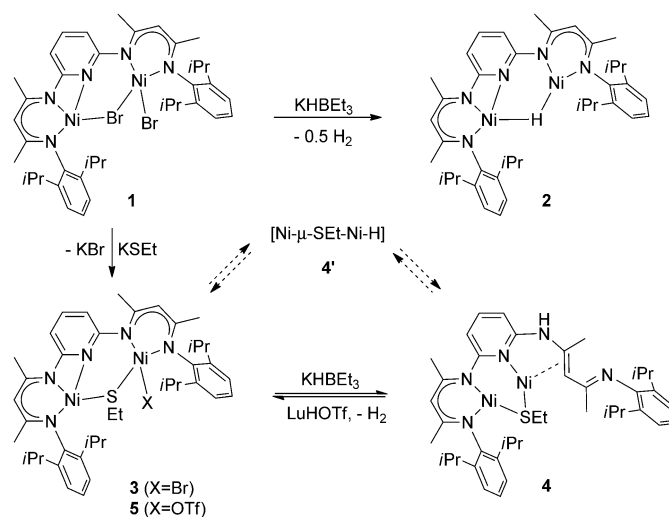
that the magnetic moment of complex **1** results from the tetrahedrally coordinated Ni^{II} atom, whilst all of the spins on the Ni^I atom with a distorted square-planar ligand arrangement are paired.

The ¹H NMR resonances are relatively sharp, but they are paramagnetically shifted over a wide range from $\delta = +50$ to -50 ppm. A resonance set was observed that was characteristic of a symmetrical complex (see the Supporting Information), which may be explained by a dynamic behaviour of the terminal bromide ligand, that is, by its fast shift on the NMR timescale. Cooling an NMR sample to -70°C ($[\text{D}_8]\text{toluene}$) led to several changes. However, because these changes included a significant broadening and shifting of resonances, a straightforward interpretation in terms of decoalescence was not possible.

Dinickel complex **1** represents a suitable starting material for the synthesis of hydride compounds by its reaction with KHBET_3 or salt metathesis with other metal hydrides. A dinickel(II)–dihydride compound, similar to complex **1** (Scheme 1), was principally conceived as the product, but, the fact that, within complex **1**, one of the bromide ligands remained terminal, already indicated that a $\text{Ni}(\mu\text{-H})_2\text{Ni}$ core might not be accessible. Furthermore, complex **1** had been found to be unstable with respect to H_2 elimination in the presence of donors, such as pyridines. Because PYR-H_2 features a built-in pyridine unit, we anticipated that the use of this ligand could induce a partial loss of H_2 . Simple replacement of the two bromide ligands by hydride ligands would lead to a $\text{Ni}^{\text{II}}-\mu\text{-H}-\text{Ni}^{\text{II}}-\text{H}$ moiety, which resembles the $\text{Fe}^{\text{II}}-\mu\text{-H}-\text{Ni}^{\text{III}}-\text{H}$ intermediate that has been proposed for the $[\text{NiFe}]$ hydrogenase in a theoretical study.^[10,15] This latter structure represents an energy maximum within the system and releases a proton and an electron to give $\text{Fe}^{\text{II}}-\mu\text{-H}-\text{Ni}^{\text{II}}$ in an exothermic process. There is not much precedent for $\text{Ni}^{\text{II}}-\mu\text{-H}-\text{Ni}^{\text{II}}-\text{H}$ entities in molecular chemistry, although a few examples are known: $[(\text{dippe})_2\text{Ni}_2\text{H}_3][\text{PPh}_4]$, $[(\text{dcype})_2\text{Ni}_2\text{H}_3][\text{PPh}_4]$, and $[(\text{dippe})_2\text{Ni}_2(\text{H})_3][\text{BEt}_4]$ ($\text{dippe} = 1,2\text{-bis}(\text{diisopropylphosphino})\text{-ethane}$, $\text{dcype} = 1,2\text{-bis}(\text{dicyclohexylphosphino})\text{ethane}$).^[16]

Adding KHBET_3 to a solution of compound **1** in toluene immediately led to a colour change from green to red, accompanied by the appearance of an absorption band at 560 nm in the UV/Vis spectrum (see the Supporting Information). Subsequent work-up led to a dinuclear $\text{Ni}^{\text{II}}\text{Ni}^{\text{I}}$ complex, $[(\text{PYR})\text{Ni}(\mu\text{-H})\text{Ni}]$ (**2**), as red crystals, which featured a bridging hydride ligand between the metal centres (Scheme 3). Perhaps, first of all, a $\text{Ni}^{\text{II}}-\mu\text{-H}-\text{Ni}^{\text{II}}-\text{H}$ complex had formed, as suggested above. However, because the β -diketiminato ligand stabilises the Ni^{I} oxidation state, the system prefers to eliminate a H atom in the form of H_2 , which could be detected (see the Supporting Information).

Crystals suitable for X-ray diffraction could be obtained by the slow evaporation of the solvent from a solution in Et_2O . The molecular structure of compound **2** shows that one of the two nickel centres is surrounded by its ligands in a distorted square-planar fashion, whereas the second one is located in a trigonal coordination sphere. The bridging hy-



Scheme 3. Synthesis of $\text{Ni}^{\text{I}}\text{Ni}^{\text{II}}-\text{H}$ complex **2** and $\text{Ni}^{\text{I}}-\mu\text{-SEt}-\text{Ni}^{\text{I}}$ complex **4** ($\text{LuHOTf} = \text{lutidinium triflate}$).

dride ligand between the two nickel centres was found in the difference Fourier map. The $\text{Ni}^{\text{I}}-\text{H}1$ distance ($1.50(2) \text{ \AA}$) is similar to previously reported $\text{Ni}^{\text{II}}-\text{H}$ distances for $\text{Ni}^{\text{II}}-\text{H}$ units in a square-planar coordination environment (e.g., $1.49(5)$, $1.43(5)$, and $1.505(20) \text{ \AA}$),^[11,17] whilst the $\text{Ni}^{\text{II}}-\text{H}1$ bond is somewhat longer ($1.62(2) \text{ \AA}$). The $\text{Ni}-\text{Ni}$ distance ($2.5966(3) \text{ \AA}$) is much shorter than the corresponding one in complex **1** ($3.4290(7) \text{ \AA}$). However, DFT calculations ($\text{B3LYP/Def2-SVP/TZVPD}$,^[18] see the Supporting Information) excluded a $\text{Ni}\cdots\text{Ni}$ bonding interaction and revealed that the nature of the $\text{Ni}^{\text{II}}-\mu\text{-H}-\text{Ni}^{\text{I}}$ moiety is not as straightforward as Figure 2 may suggest. Rather, it should be viewed as a $\text{Ni}^{\text{II}}-\text{H}$ unit that is coordinated to a Ni^{I} ion, that is, as a $\text{Ni}^{\text{II}}-\text{H}\rightarrow\text{Ni}^{\text{I}}$ moiety, which also explains the observed $\text{Ni}-\text{H}$ bond lengths.

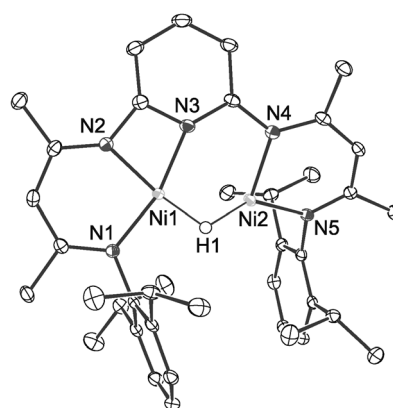


Figure 2. Molecular structure of complex **2**; ellipsoids are set at 50% probability. Hydrogen atoms, beside the bridging hydride atoms, are omitted for clarity. Selected bond lengths [\AA] and angles [$^\circ$]: $\text{Ni}1-\text{Ni}1$ $1.8800(13)$, $\text{Ni}2-\text{Ni}1$ $1.8586(14)$, $\text{Ni}3-\text{Ni}1$ $1.9049(13)$, $\text{Ni}1-\text{Ni}2$ $2.5966(3)$, $\text{Ni}2-\text{N}4$ $1.9493(14)$, $\text{Ni}2-\text{N}5$ $1.8946(13)$, $\text{Ni}2-\text{N}3$ $2.7449(14)$, $\text{Ni}1-\text{H}1$ $1.50(2)$, $\text{Ni}2-\text{H}1$ $1.62(2)$; $\text{Ni}1-\text{Ni}1-\text{N}2$ $94.62(6)$, $\text{N}4-\text{Ni}2-\text{N}5$ $96.33(6)$.

As in complex **1**, the square-planar-coordinated Ni1 atom can be expected to be in the low-spin state ($S=0$), whereas the Ni2 atom contains one unpaired electron (as confirmed by DFT calculations). Correspondingly, the magnetic moment of complex **2** was found to be $\mu_{\text{eff}}=1.82 \mu_{\text{B}}$ ($\mu_{\text{s.o.}}=1.73 \mu_{\text{B}}$) at room temperature (Evans method). This result is in accordance with the EPR spectrum that was recorded for a solution after cooling to 77 K, which showed a rhombic signal ($g_x=2.054$, $g_y=2.159$, $g_z=2.454$) that is typical for Ni^I compounds with one unpaired electron ($S=1/2$; Figure 3).^[19]

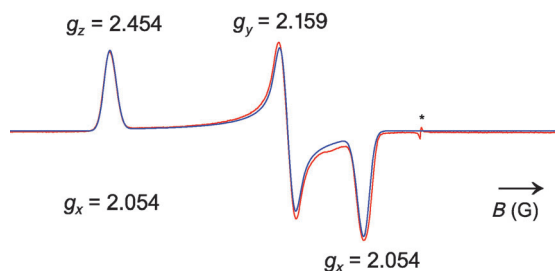


Figure 3. EPR spectrum of complex **2** in toluene at 77 K. Red: Experimental spectrum with MgO/Cr³⁺ (*) as an internal standard; blue: Powder simulation with the indicated g values.

Within the active site of [NiFe] hydrogenase, the nickel centre is in a cysteinyl environment, which presumably aids the redox transformations. Hence, we envisaged introducing a thiolate ligand into the [(PYR)Ni₂]²⁺ system prior to hydride transfer. This goal was achieved by the reaction of compound **1** with KSEt, which led to a selective replacement of the bridging bromide by a thiolate ligand and, thus, to complex [(PYR)Ni(μ-SEt)NiBr] (**3**; Scheme 3), whose molecular structure is shown in Figure 4.

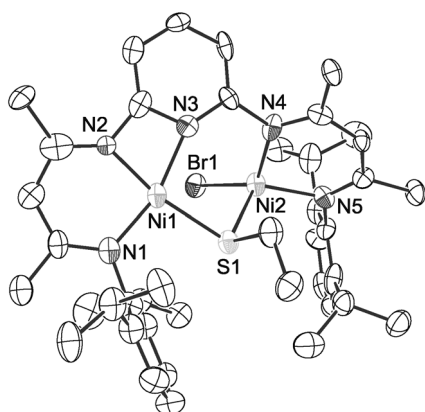


Figure 4. Molecular structure of complex **3**-toluene; ellipsoids are set at 50% probability. The non-coordinating toluene molecule in the unit cell and the hydrogen atoms are omitted for clarity. Selected bond lengths [Å] and angles [°]: N1–Ni1 1.895(3), N2–Ni1 1.858(3), N3–Ni1 1.960(3), Ni1–S1 2.2355(10), Ni1–Ni2 3.2072(7), Ni2–S1 2.2715(10), Ni2–Br1 2.3764(6), Ni2–N4 1.958(3), Ni2–N5 1.952(3), Ni2–N3 2.9536(19); N1–Ni1–N2 93.58(13), N4–Ni2–N5 94.40(12), S1–Ni2–Br1 103.99(3), Br1–Ni2–N4 125.83(9), N5–Ni2–S1 111.26(9).

As in complex **1**, one of the nickel centres adopts a square-planar coordination geometry, whilst the other one is surrounded by its ligands distorted tetrahedrally. The magnetic moment for its solution in [D₆]benzene at room temperature, $\mu_{\text{eff}}=3.06 \mu_{\text{B}}$, is typical for tetrahedral $S=1$ nickel systems ($\mu_{\text{s.o.}}=2.83 \mu_{\text{B}}$). DFT calculations confirmed the $S=1$ ground state of complex **3**. Analysis of a solution in MeCN by mass spectrometry (ESI) showed a signal at m/z 766.2951, which corresponded to $[M-\text{Br}]^+$, with a characteristic isotopic distribution that matched the calculated isotopic distribution (see the Supporting Information).

Consequently, in the next step, we attempted to replace the remaining bromide ligand in complex **3** by a hydride ligand. Indeed, an EXD investigation on the product of the reaction between complex **3** and KHBE₃ confirmed the absence of bromide, indicating a conversion as envisaged. However, as subsequently revealed by single-crystal X-ray diffraction analysis (Figure 5) the expected hydride com-

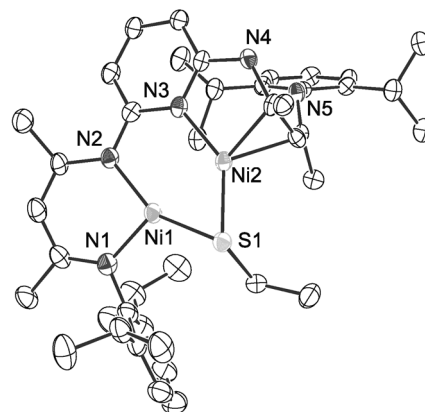


Figure 5. Molecular structure of complex **4**-*n*-hexane; ellipsoids are set at 50% probability. The non-coordinating *n*-hexane molecule in the unit cell and the hydrogen atoms are omitted for clarity. Selected bond lengths [Å] and angles [°]: N1–Ni1 1.888(5), N2–Ni1 1.896(4), N3–Ni1 2.9174(4), Ni1–S1 2.1131(13), Ni1–Ni2 2.3619(9), Ni2–N3 1.914(4), Ni2–C15 2.059(5), Ni2–C16 2.032(5), Ni2–S1 2.1471(14); N1–Ni1–N2 93.35(14), Ni1–S1–Ni2 67.34(4).

plex, [(PYR-H)Ni(μ-SEt)NiH] (**4'**; Scheme 3), had not formed; rather, an isomer, [(PYR-H)Ni(μ-SEt)Ni] (**4**), was obtained, which could formally be derived from complex **4'** through the following process: 1) Heterolytic cleavage of the initially formed Ni^{II}–H bond into H⁺ and Ni⁰; 2) protonation of one diketiminato binding pocket with the removal of Ni⁰; 3) coordination of Ni⁰ onto the pyridyl unit and the formation of a Ni^INi^I core after interaction with the remaining Ni^{II} ion; 4) saturation of the coordination sphere of the released Ni centre by a C=C unit of the diketimine. Altogether, the reaction may be compared to the reduction of a nickel centre by a hydride, with the concomitant trapping of H⁺ by a pendant base, as observed by DuBois and co-workers.^[2b, 4g, 20]

The Ni–Ni distance in complex **4** is 2.3619(9) Å, which is much shorter than that in the other complexes (**1–3**). Com-

paring this nickel–nickel separation to that in other related Ni^I complexes suggests an analogous interpretation of its structures in terms of a Ni^I–Ni^I bond.^[21] To evaluate the bonding situation in complex **4**, DFT calculations were performed (B3LYP/Def2-SVP/TZVPD,^[18] see the Supporting Information). A broken-symmetry singlet state with two Ni^I ions was found to be the ground state, wherein the two unpaired electrons of the Ni ions are coupled antiferromagnetically. The corresponding triplet state and the closed-shell singlet state (with one Ni^{II} and one Ni⁰ centre) are positioned 16 and 22 kJ mol⁻¹ higher in energy than the ground state, respectively. Hence, although there is no bonding interaction between both nickel ions, their unpaired electrons exhibit strong antiferromagnetic coupling, so that compound **4** shows diamagnetic character, thus leading to a sharp set of signals in the diamagnetic range of the ¹H NMR spectrum (see the Supporting Information). To detect the formation of any hydride intermediates, the reaction of complex **3** with KHBET₃ was carried out at –70 °C in [D₈]toluene and monitored by NMR spectroscopy. Indeed, the reaction began immediately, but the spectrum of paramagnetic complex **3** changed into that of a further paramagnetic species, which changed upon warming until, finally, the spectrum of diamagnetic complex **4** was obtained. The broad, paramagnetic signals that were observed in between these two states did not allow for a reasonable interpretation.

As a consequence of the short Ni–Ni distance, the Ni–S bonds in complex **4** are shorter (Ni1–S1 2.1131(13) Å, Ni2–S1 2.1471(14) Å) than those in complex **3** (Ni1–S1 2.2355(10) and Ni2–S1 2.2715(10) Å). The N3–Ni1 separation is very large (2.9174(45) Å), whilst the Ni2–N3 distance (1.914(4) Å) compares well with the N3–Ni1 distances in complexes **1–3** (1.950(2), 1.9049(13), and 1.960(3) Å).

Having “loaded” the [(PYR)Ni(μ-SEt)Ni]⁺ system with hydride, which led to internal redox chemistry, the question was how the reduced core behaved upon protonation. After the addition of lutidinium triflate as a mild acid to a solution of compound **4** in THF, Ni^{II}Ni^{II} complex [(PYR)Ni(μ-SEt)Ni(OTf)] (**5**) was isolated, which is the triflate derivative of complex **3** (Scheme 3). It is likely that, first of all, the proton attacked the Ni^INi^I core, thereby leading to a Ni^{II}Ni^{II}H unit, based on precedence for this reaction in the literature.^[4j,22] However, the hydride ligand then combined with the proton at the protonated β-diketiminato site to yield H₂.

Hence, altogether, a dinickel system is described in which hydride can be stepwise separated into a proton and electrons (→**4**) that, on the addition of a proton, are recombined to give H₂. The molecular structure of complex **5** is comparable to that of the starting compound (**3**), but, instead of the terminal bromide, a triflate ion is bound to the Ni2 atom in complex **5** (Figure 6). As in complexes **2** and **3**, the coordination sphere of one nickel ion is almost square-planar, whereas the other one is coordinated in a distorted tetrahedral geometry; thus, again, a *S* = 1 ground state was expected and, indeed, a $\mu_{\text{eff}} = 2.50 \mu_{\text{B}}$ magnetic moment was determined for solid complex **5** at 295 K ($\mu_{\text{s.o.}} = 2.83 \mu_{\text{B}}$).

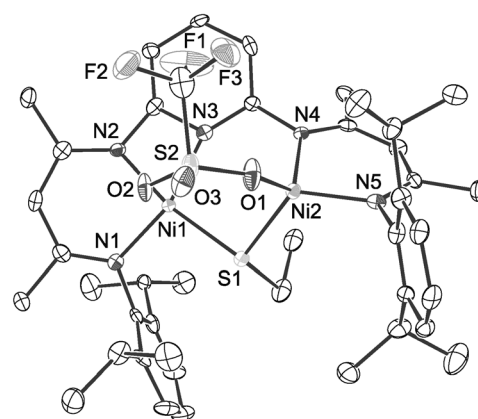


Figure 6. Molecular structure of complex **5**; ellipsoids are set at 50% probability. Hydrogen atoms are omitted for clarity. Selected bond lengths [Å] and angles [°]: Ni1–Ni1 1.895(5), Ni2–Ni1 1.834(5), N3–Ni1 1.955(5), Ni1–S1 2.2209(18), Ni1–Ni2 3.3485(11), Ni2–N3 2.990(4), Ni2–N4 1.925(5), Ni2–N5 1.943(5), Ni2–S1 2.2637(16), Ni2–O1 2.008(4); N1–Ni1–N2 93.4(2), Ni1–S1–Ni2 96.60(7), N4–Ni2–N5 95.75(19).

However, its NMR spectra in C₆D₆ indicated diamagnetic behaviour and, thus, spin-pairing in solution. To rationalise this finding, DFT calculations were also carried out for complex **5**: Setting out with the results of the X-ray diffraction analysis, a single-point calculation revealed a preference for a triplet state, whilst geometry optimisation led to a structure in which two high-spin Ni^{II} centres are strongly antiferromagnetically coupled so that the molecule has a singlet ground state. This result explains the diamagnetic character of complex **5** on the basis that the structure relaxation that was observed in the calculations also occurs upon the dissolution of solid complex **5**.

It should be emphasised that the formation of complexes **2**, **4**, and **5** proceeds in a very clean manner: The yields of the crystalline products are all at least 60% and analysis of the crude products revealed even higher (almost quantitative) conversion. Consequently, these findings show that, within the [(PYR)Ni₂]²⁺ framework, the ligand that bridges the two nickel centres sensitively influences its electronic structure. Thus, this ligand also determines the redox chemistry that is triggered by the presence of hydride ligands. In case of a thiolate ligand, this chemistry led to complex **4**, which will be in the focus of future studies: Examples of thiolate-bridged dinuclear nickel(I) compounds are rare^[21a] and complex **4** is highly reactive; thus, it will be interesting to explore its potential, for instance, in mediating redox coupling reactions.

Conclusion

We have shown that the PYR²⁻ ligand is able to coordinate two nickel(II)–bromide moieties, thereby affording a Ni^{II}–μ-Br–Ni^{II}–Br core. In a subsequent reaction with KHBET₃, the bromide ligands are replaced by hydride ligands, but the Ni^{II}–μ-H–Ni^{II}–H product, which is likely formed initially, is

unstable with respect to H₂ elimination so that, finally, a Ni^I-μ-H-Ni^{II} complex is isolated. If the bridging bromide ligand is replaced by a thiolate unit prior to the reaction with KHBET₃, the product formation takes a different course. It is assumed that, first of all, a bromide/hydride exchange takes place, which would lead to a Ni^{II}-μ-SEt-Ni^{II}-H species. In contrast to the observation made when setting out with an all-bromide system, further reaction does not proceed through the elimination of H⁺ (→H₂) but, instead, proceeds through a process that may be formally viewed as a reduction of the metal centres by the hydride ligand.^[20] Its two electrons reduce both Ni^{II} centres to an oxidation state of +I, whilst the proton is trapped by a basic site on the ligand. Interestingly, the split hydride can be removed from compound **4** again by the addition of a mild acid, thereby regenerating a core that is comparable to that in complex **3**. Future investigations will concern the reactivity of compound **4** with H₂/H⁺/e⁻, that is, the substrates of [NiFe] hydrogenase.

Experimental Section

General: All manipulations were carried out under an argon atmosphere in dried glassware in a glove box or by using standard Schlenk techniques. Solvents were dried by using an MBraun Solvent Purification System (SPS). The ¹H and ¹³C NMR spectra were recorded on a Bruker AV 400 NMR spectrometer at 25 °C. ¹H and ¹³C chemical shifts are reported in ppm and were calibrated internally to the solvent signals (C₆D₆: δ = 7.15 and 128.02 ppm, respectively). The coupling constants are given in Hz. IR spectra were measured as KBr pellets on a Shimadzu FTIR 8400S spectrometer. UV/Vis spectroscopy was performed on a HP8453A diode-array spectrometer. HRMS (ESI) was recorded on an Agilent 6210 time-of-flight instrument. Elemental analysis was performed on a HEKAtech Euro EA 3000 elemental analyzer. The Evans method was used to determine the magnetic moments in solution at RT;^[23] the samples were measured in C₆D₆ with 1% tetramethylsilane (TMS), together with a capillary tube that contained C₆D₆ with 1% TMS as an internal standard. Different susceptibility measurements led to different shifts of the TMS resonances. The magnetic moment of a solid sample was determined by using a magnetic balance (Alfa) at RT. For the diamagnetic correction of the susceptibility, Pascal's constants were used.^[24] EPR spectroscopy was carried out in silica glass tubes on an ERS 300 X-band EPR spectrometer at 9.2 GHz. The ligand PYR-H₂ was prepared according to a literature procedure.^[12a]

[(PYR)Ni(μ-Br)NiBr] (1): A solution of PYR-H₂ (2.64 g, 4.47 mmol) in THF (30 mL) was cooled to -78 °C and *n*BuLi (2 equiv, 3.57 mL, 8.93 mmol, 2.5 M in *n*-hexane) was added. After stirring for 15 min at RT, the solution was added to a suspension of [NiBr₂(dme)] (2 equiv, 2.76 g, 8.93 mmol) in THF (20 mL) and the mixture was stirred for 16 h. After filtration of the dark-green solution, the solvent was removed in vacuo. The residue was extracted with toluene (15 mL) and layered with *n*-hexane (10 mL). Cooling to -30 °C afforded complex **1** as dark-green crystals (2.15 g, 56% yield). ¹H NMR (400 MHz, C₆D₆, 25 °C): δ = 42.15 (1H; CH_{4-Pyr}), 19.35 (4H; CH_{Ar}), 1.73 (12H; CH(CH₃)₂), -0.05 (12H; CH(CH₃)₂), -7.63 (2H; CH_{3.5-Pyr}), -10.30 (2H; CH_{Ar}), -12.96 (6H; CH₃), -19.67 (6H; CH₃), -41.48 ppm (2H; CH); IR (KBr): $\tilde{\nu}$ = 3056 (w), 2962 (s), 2926 (m), 2865 (m), 1596 (s), 1573 (s), 1550 (vs), 1517 (s), 1455 (s), 1437 (s), 1410 (vs), 1394 (vs), 1372 (vs), 1339 (s), 1319 (s), 1302 (s), 1282 (vs), 1254 (m), 1228 (s), 1186 (m), 1158 (s), 1107 (w), 1055 (w), 1026 (m), 934 (w), 837 (w), 797 (m), 762 (m), 731 (w), 632 (w), 532 cm⁻¹ (w); UV/Vis (toluene): λ_{max} (ε) = 470 (8150), 612 (450), 662 nm (315 mol⁻¹ dm³ cm⁻¹); μ_{eff} = 3.03 μ_B (295 K, μ_{so} = 2.83 μ_B); elemental anal-

ysis calcd (%) for C₃₉H₅₁Br₂N₅Ni₂: C 54.02, H 5.93, N 8.01; found: C 54.61, H 5.92, N 7.90.

[(PYR)Ni(μ-H)Ni] (2): [(PYR)Ni₂Br₂] (400 mg, 0.461 mmol) was dissolved in Et₂O (40 mL) and a solution of KHBET₃ (2 equiv, 127 mg, 0.923 mmol) in Et₂O (10 mL) was added. After stirring for 5 min at RT, the solvent was removed in vacuo. The residue was extracted with toluene (20 mL) and evaporation of the solvent yielded complex **2** as a red solid (205 mg, 63% yield). IR (KBr): $\tilde{\nu}$ = 3573 (w), 3419 (m), 3058 (w), 2960 (s), 2925 (m), 2867 (m), 1628 (m), 1539 (s), 1457 (s), 1437 (s), 1378 (vs), 1321 (s), 1224 (m), 1187 (m), 1160 (m), 1056 (m), 760 cm⁻¹ (m); UV/Vis (toluene): λ_{max} (ε) = 455 (6830), 560 nm (1500 mol⁻¹ dm³ cm⁻¹); μ_{eff} = 1.82 μ_B (295 K, μ_{so} = 1.73 μ_B); elemental analysis calcd (%) for C₃₉H₅₂N₅Ni₂: C 66.13, H 7.40, N 9.89; found: C 65.30, H 7.25, N 9.42.

[(PYR)Ni(μ-SEt)NiBr] (3): A solution of complex **1** (400 mg, 0.461 mmol) in THF (40 mL) was treated with KSET (1 equiv, 46.0 mg, 0.461 mmol) and the mixture was stirred for 16 h at RT. After filtration of the green-brown solution, the solvent was removed in vacuo. The residue was extracted with toluene (20 mL) and evaporation of the solvent afforded complex **3** as a brown solid (310 mg, 80% yield). IR (KBr): $\tilde{\nu}$ = 3058 (w), 2959 (s), 2924 (m), 2867 (m), 1755 (w), 1595 (s), 1543 (vs), 1526 (s), 1455 (s), 1437 (s), 1406 (vs), 1392 (vs), 1364 (vs), 1339 (s), 1319 (s), 1285 (s), 1300 (s), 1260 (m), 1229 (m), 1223 (m), 1184 (m), 1162 (m), 1099 (m), 1056 (m), 1029 (s), 957 (w), 937 (w), 859 (w), 796 (s), 761 (s), 727 (w), 713 (w), 677 (w), 629 (w), 543 (w), 519 cm⁻¹ (w); μ_{eff} = 3.06 μ_B (295 K, μ_{so} = 2.83 μ_B); HRMS (ESI): *m/z* calcd for [C₄₁H₅₆N₅Ni₂S]⁺: 766.2963 [M-Br]⁺; found: 766.2951; elemental analysis calcd (%) for C₄₁H₅₆BrN₅Ni₂S: C 58.05, H 6.65, N 8.26, S 3.78; found: C 58.43, H 6.63, N 8.21, S 3.44.

[(PYR-H)Ni(μ-SEt)Ni] (4): A solution of KHBET₃ (1 equiv, 15.8 mg, 0.114 mmol) in Et₂O (5 mL) was added to a solution of complex **3** (100 mg, 0.114 mmol) in Et₂O (15 mL). The mixture was stirred for 15 min at RT and the solvent was removed in vacuo. The residue was extracted with *n*-hexane (10 mL) and evaporation of the solvent yielded complex **4** as a brown-red solid (62.5 mg, 71% yield). ¹H NMR (400 MHz, C₆D₆, 25 °C): δ = 8.92 (s, 1H; NH), 7.15 (m, 6H; CH_{Ar}), 6.58 (t, ³J = 7.6 Hz, 1H; CH_{4-Pyr}), 5.76 (d, ³J = 7.6 Hz, 1H; CH_{3.5-Pyr}), 5.64 (d, ³J = 7.6 Hz, 1H; CH_{3.5-Pyr}), 5.02 (s, 1H; CH), 4.98 (s, 1H; CH), 4.21 (m, 1H; CH(CH₃)₂), 3.81 (m, 1H; CH(CH₃)₂), 2.87 (m, 2H; CH(CH₃)₂), 2.12 (d, ³J = 6.4 Hz, 3H; CH(CH₃)₂), 2.03 (s, 3H; CH₃), 1.89 (s, 3H; CH₃), 1.80 (m, 2H; SCH₂), 1.69 (s, 3H; CH₃), 1.63 (d, ³J = 6.4 Hz, 3H; CH(CH₃)₂), 1.51 (d, ³J = 6.8 Hz, 3H; CH(CH₃)₂), 1.44 (s, 3H; CH₃), 1.18 (d, ³J = 6.4 Hz, 3H; CH(CH₃)₂), 1.17 (d, ³J = 6.0 Hz, 3H; CH(CH₃)₂), 1.00 (d, ³J = 6.8 Hz, 3H; CH(CH₃)₂), 0.84 ppm (m, 3H; SCH₃); ¹³C NMR (100 MHz, C₆D₆, 25 °C): δ = 169.3 (1C; C), 168.6 (1C; C), 162.5 (1C; C), 154.3 (1C; C), 151.1 (1C; C), 146.5 (1C; C), 140.5 (1C; C), 139.5 (1C; C), 138.5 (1C; CH_{4-Pyr}), 137.0 (1C; C), 136.5 (1C; C), 124.9 (1C; CH_{Ar}), 124.1 (2C; CH_{Ar}), 123.3 (C; CH_{Ar}), 123.3 (1C; CH_{Ar}), 122.9 (1C; CH_{Ar}), 112.0 (1C; C), 109.7 (1C; CH_{3.5-Pyr}), 106.8 (1C; CH), 103.6 (1C; CH_{3.5-Pyr}), 28.6 (1C; CH(CH₃)₂), 28.6 (3C; CH(CH₃)₂), 27.8 (1C; SCH₂), 25.3 (1C; CH(CH₃)₂), 25.3 (1C; CH₃), 24.8 (1C; CH(CH₃)₂), 24.0 (1C; CH(CH₃)₂), 23.9 (1C; CH(CH₃)₂), 23.9 (1C; CH(CH₃)₂), 23.7 (1C; CH₃), 23.4 (1C; CH(CH₃)₂), 23.3 (1C; CH(CH₃)₂), 23.0 (1C; CH(CH₃)₂), 22.6 (1C; CH₃), 22.3 (1C; CH₃), 18.1 ppm (1C; SCH₃); IR (KBr): $\tilde{\nu}$ = 3062 (w), 2961 (s), 2924 (m), 2865 (m), 1610 (m), 1560 (s), 1510 (m), 1437 (s), 1384 (vs), 1320 (s), 1261 (vs), 1186 (s), 1157 (s), 1099 (s), 1056 (m), 1027 (s), 986 (m), 936 (w), 865 (w), 798 cm⁻¹ (s); elemental analysis calcd (%) for C₄₁H₅₇N₅Ni₂S: C 64.00, H 7.47, N 9.10, S 4.17; found: C 63.82, H 7.60, N 8.56, S 3.29.

[(PYR)Ni(μ-SEt)Ni(OTf)] (5): A solution of [(PYR-H)Ni(μ-SEt)Ni] (25.0 mg, 0.033 mmol) in THF (5 mL) was treated with a solution of lutidinium triflate (8.40 mg, 0.033 mmol) in THF (2 mL) and the reaction mixture was stirred for 5 min at RT. The solvent was removed in vacuo and the residue was extracted with Et₂O. Evaporation of the solvent yielded compound **5** as a dark-red solid (18.5 mg, 60% yield). ¹H NMR (400 MHz, C₆D₆, 25 °C): δ = 7.04 (m, 6H; CH_{3.5-Pyr}, CH_{Ar}), 6.85 (t, ³J = 7.8 Hz, 1H; CH_{4-Pyr}), 6.57 (t, ³J = 7.8 Hz, 1H; CH_{4-Pyr}), 6.36 (d, ³J = 7.2 Hz, 2H; CH_{Ar}), 5.48 (d, ³J = 6.9 Hz, 1H; CH_{3.5-Pyr}), 4.97 (s, 1H; CH), 4.95 (s, 1H; CH), 3.95 (m, 1H; CH(CH₃)₂), 3.73 (m, 1H; CH(CH₃)₂), 3.11 (m,

1H; CH(CH₃)₂, 2.95 (m, 1H; CH(CH₃)₂), 2.32 (s, 6H; CH₃), 1.89 (s, 3H; CH₃), 1.81 (m, 2H; SCH₂), 1.45 (d, ³J=6.9 Hz, 3H; CH(CH₃)₂), 1.37 (m, 9H; CH₃, CH(CH₃)₂), 1.13 (m, 6H; CH(CH₃)₂), 1.08 (d, ³J=6.3 Hz, 3H; CH(CH₃)₂), 0.92 (d, ³J=6.6 Hz, 3H; CH(CH₃)₂), 0.76 ppm (t, ³J=7.5 Hz, 3H; SCH₂); IR (KBr): $\tilde{\nu}$ =3129 (w), 3058 (w), 2963 (s), 2927 (m), 2867 (m), 1594 (s), 1541 (vs), 1459 (s), 1437 (s), 1409 (s), 1391 (vs), 1364 (vs), 1339 (s), 1317 (vs), 1299 (s), 1281 (s), 1254 (m), 1231 (s), 1210 (s), 1181 (s), 1164 (s), 1108 (m), 1097 (m), 1055 (m), 1026 (s), 958 (w), 942 (w), 933 (w), 834 (w), 793 (m), 761 (m), 732 (w), 715 (w), 680 (w), 634 (s), 586 (w), 515 cm⁻¹ (w); μ_{eff} =2.50 μ_{B} (solid, 295 K, $\mu_{\text{calc.}}$ =2.83 μ_{B}); HRMS (ESI): *m/z* calculated for [C₄₁H₅₆N₃Ni₂S]⁺: 766.2963 [M-OTf]⁺; found: 766.2965; elemental analysis calcd (%) for C₄₂H₅₆F₃N₃Ni₂O₃S₂: C 54.98, H 6.15, N 7.63, S 6.99; found: C 55.69, H 6.27, N 8.08, S 5.51.

Crystallographic studies: Crystallographic data were collected on a STOE IPDS 2T diffractometer at 100 K by using MoK α radiation (λ =0.71073 Å). The structures were solved by using direct methods with SHELXS-97 and refined by using full-matrix least-squares with SHELXL-97.^[25] All non-hydrogen atoms were refined anisotropically. Hydrogen atoms were added geometrically and refined by using a riding model; in complex **2**, the bridging hydride atom was located in the difference Fourier map. Numerical absorption correction was applied for complexes **1** and **3**, based on a Gaussian algorithm, which was implemented in the X-RED program (Stoe, 2002). Owing to thermal motion, the ethyl-thiolate group in complex **5** was found to be disordered over two sites. The 1–2 and 1–3 distances of the disordered parts were restrained to be similar by using the EADP and DFIX commands. For the disordered toluene molecule in the unit cell of complex **3**, the SADI instruction was applied and all of the atoms of the disordered solvent molecule were forced into a plane by using the FLAT command. The restraints DELU and EADP were applied to the solvent molecule that was incorporated into the unit cell of complex **4**.

CCDC-891189 (**1**), CCDC-891190 (**2**), CCDC-891191 (**3**), CCDC-891192 (**4**), and CCDC-891193 (**5**) contain the supplementary crystallographic data for this paper. These data can be obtained free of charge from The Cambridge Crystallographic Data Centre via www.ccdc.cam.ac.uk/data_request/cif.

Crystal data for complex 1. C₃₀H₅₁Br₂N₃Ni₂; *M_w*=867.09; monoclinic; space group *P*₂/*c*; *a*=13.9183(17), *b*=12.0355(11), *c*=23.810(2) Å; α =90, β =100.251(9), γ =90°; *V*=3924.8(7) Å³; *T*=100 K; *Z*=4; 37 161 reflections measured; 7303 unique reflections (*R*_{int}=0.1347); final *R* indices [*I*>2 σ (*I*)] *R*₁=0.0436 and *wR*₂=0.1101; *R* indices (all data) *R*₁=0.0497 and *wR*₂=0.1136.

Crystal data for complex 2. Slow evaporation of a solution in Et₂O yielded complex **2** as red crystals. C₃₉H₅₂N₃Ni₂; *M_w*=708.28; triclinic; space group *P*-1; *a*=8.8433(5), *b*=12.2811(7), *c*=17.3724(10) Å; α =105.382(4), β =95.104(4), γ =102.044(4)°; *V*=1758.15(17) Å³; *T*=100 K; *Z*=2; 18557 reflections measured; 6888 unique reflections (*R*_{int}=0.0498); final *R* indices [*I*>2 σ (*I*)] *R*₁=0.0277 and *wR*₂=0.0658; *R* indices (all data) *R*₁=0.0340 and *wR*₂=0.0681.

Crystal data for complex 3. Brown crystals of complex **3** were obtained by layering a solution in toluene with *n*-hexane and cooling to -30°C. C₆₉H₁₂₀N₁₀Ni₄S₂; *M_w*=1788.73; triclinic; space group *P*-1; *a*=10.3265(14), *b*=12.0614(19), *c*=18.755(4) Å; α =97.814(16), β =103.849(15), γ =103.516(12)°; *V*=2159.2(7) Å³; *T*=100 K; *Z*=1; 20469 reflections measured; unique reflections (*R*_{int}=0.1419); final *R* indices [*I*>2 σ (*I*)] *R*₁=0.0501 and *wR*₂=0.1442; *R* indices (all data) *R*₁=0.0579 and *wR*₂=0.1504.

Crystal data for complex 4. Red-brown crystals of complex **4** were obtained after slow evaporation of a solution *n*-hexane. C₄₇H₇₀N₃Ni₂S; *M_w*=854.56; triclinic; space group *P*-1; *a*=9.1306(6), *b*=12.6216(12), *c*=20.4084(15) Å; α =90.694(7), β =102.437(6), γ =98.116(7)°; *V*=2271.5(3) Å³; *T*=100 K; *Z*=2; 18 121 reflections measured; 8176 unique reflections (*R*_{int}=0.1155); final *R* indices [*I*>2 σ (*I*)] *R*₁=0.0661 and *wR*₂=0.1415; *R* indices (all data) *R*₁=0.1164 and *wR*₂=0.1632.

Crystal data for complex 5. Black crystals of compound **5** were obtained after the evaporation of a solution in Et₂O. C₄₂H₅₆F₃N₃Ni₂O₃S₂; *M_w*=917.46; monoclinic; space group *P*₂/*c*; *a*=13.8476(11), *b*=12.2518(8), *c*=25.368(3) Å; α =90, β =97.774(9), γ =90°; *V*=4264.3(7) Å³; *T*=

100 K; *Z*=4; 18 121 reflections measured; 21 882 unique reflections (*R*_{int}=0.1607); final *R* indices [*I*>2 σ (*I*)] *R*₁=0.0700 and *wR*₂=0.1011; *R* indices (all data) *R*₁=0.1395 and *wR*₂=0.1180.

Acknowledgements

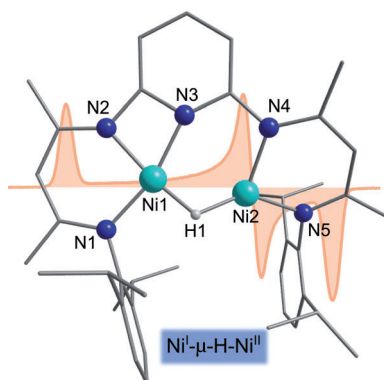
We are grateful to the Cluster of Excellence “Unifying Concepts in Catalysis”, which is funded by the Deutsche Forschungsgemeinschaft (DFG), the Fonds der Chemischen Industrie, and the Humboldt-Universität zu Berlin for financial support.

- For example, see: a) R. Kokes, *J. Am. Chem. Soc.* **1959**, *81*, 5032–5037; b) M. Sakai, N. Hirano, F. Harada, Y. Sakakibara, N. Uchino, *Bull. Chem. Soc. Jpn.* **1987**, *60*, 2923–2926; c) E. Kogut, A. Zeller, T. H. Warren, T. Strassner, *J. Am. Chem. Soc.* **2004**, *126*, 11984–11994; d) S. Chakraborty, J. Zhang, J. Krause, H. Guan, *J. Am. Chem. Soc.* **2010**, *132*, 8872–8873; e) E. E. Smith, G. Du, P. E. Fanwick, M. M. Abu-Omar, *Organometallics* **2010**, *29*, 6527–6533; f) S. Lin, M. W. Day, T. Agapie, *J. Am. Chem. Soc.* **2011**, *133*, 3828–3831; g) N. Castellanos-Blanco, M. Flores-Alamo, *Organometallics* **2012**, *31*, 680–686.
- a) T. James, L. Cai, M. Muetterter, *Inorg. Chem.* **1996**, *35*, 4148–4161; b) A. D. Wilson, R. K. Shoemaker, A. Miedaner, J. T. Muckerman, D. L. DuBois, M. R. DuBois, *Proc. Natl. Acad. Sci. USA* **2007**, *104*, 6951–6956; c) I. Dance, *Dalton Trans.* **2010**, *39*, 2972–2983; d) S. Canaguier, M. Fontecave, V. Artero, *Eur. J. Inorg. Chem.* **2011**, 1094–1099; e) T. Matsumoto, T. Nagahama, J. Cho, T. Hizume, M. Suzuki, S. Ogo, *Angew. Chem.* **2011**, *123*, 10766–10768; *Angew. Chem. Int. Ed.* **2011**, *50*, 10578–10580; f) M. Vogt, B. de Bruin, H. Berke, M. Trincado, H. Grützmacher, *Chem. Sci.* **2011**, *2*, 723–727.
- a) M. Brecht, M. van Gastel, T. Buhrke, B. Friedrich, W. Lubitz, *J. Am. Chem. Soc.* **2003**, *125*, 13075–13083; b) C. Mealli, T. B. Rauchfuss, *Angew. Chem.* **2007**, *119*, 9100–9102; *Angew. Chem. Int. Ed.* **2007**, *46*, 8942–8944.
- a) T. Steinke, C. Gemel, M. Cokoja, M. Winter, R. Fischer, *Angew. Chem.* **2004**, *116*, 2349–2352; *Angew. Chem. Int. Ed.* **2004**, *43*, 2299–2302; b) N. D. Clement, K. J. Cavell, C. Jones, C. J. Elsevier, *Angew. Chem.* **2004**, *116*, 3933; *Angew. Chem. Int. Ed.* **2004**, *43*, 3845; c) W. Chen, S. Shimada, M. Tanaka, *J. Am. Chem. Soc.* **2004**, *126*, 8072–8073; d) Y. Journaux, V. Lozan, J. Klingele, B. Kersting, *Chem. Commun.* **2006**, 83–84; e) L. She, X. Li, H. Sun, J. Ding, M. Frey, *Organometallics* **2007**, *26*, 566–570; f) L. Liang, P. Chien, *Organometallics* **2008**, *27*, 3082–3093; g) J. Y. Yang, R. M. Bullock, W. J. Shaw, B. Twamley, K. Frazee, M. R. DuBois, D. L. DuBois, *J. Am. Chem. Soc.* **2009**, *131*, 5935–5945; h) M. F. Laird, M. Pink, N. P. Tsvetkov, H. Fan, K. G. Caulton, *Dalton Trans.* **2009**, 1283–1285; i) S. Chakraborty, J. A. Krause, H. Guan, *Organometallics* **2009**, *28*, 582–586, and references therein; j) B. E. Barton, C. M. Whaley, T. B. Rauchfuss, D. L. Gray, *J. Am. Chem. Soc.* **2009**, *131*, 6942–6943; k) S. Canaguier, M. Field, Y. Oudart, J. Pécaut, M. Fontecave, V. Artero, *Chem. Commun.* **2010**, 46, 5876–5878; l) T. He, N. P. Tsvetkov, J. G. Andino, X. Gao, B. C. Fullmer, K. G. Caulton, *J. Am. Chem. Soc.* **2010**, *132*, 910–911; m) M. T. Mock, R. G. Potter, M. J. O’Hagan, D. M. Camaioni, W. G. Dougherty, W. S. Kassel, D. L. DuBois, *Inorg. Chem.* **2011**, *50*, 11914–11928; n) C. Tsay, J. C. Peters, *Chem. Sci.* **2012**, *3*, 1313–1318.
- For oxidation states in the [NiFe] hydrogenase, compare: a) R. P. Happe, W. Roseboom, S. P. J. Albracht, *Eur. J. Biochem.* **2001**, *259*, 602–608; b) M. Stein, W. Lubitz, *J. Inorg. Biochem.* **2004**, *98*, 862–877.
- For example, see: a) J. M. Smith, R. J. Lachicotte, K. A. Pittard, T. R. Cundari, G. Lukat-Rodgers, K. R. Rodgers, P. L. Holland, *J. Am. Chem. Soc.* **2001**, *123*, 9222–9223; b) L. Bourget-Merle, M. F. Lappert, J. R. Severn, *Chem. Rev.* **2002**, *102*, 3031–3066; c) N. W. Aboeella, S. V. Kryatov, B. F. Gherman, W. W. Brennessel, V. G. Young, R. Sarangi, E. V. Rybak-Akimova, K. O. Hodgson, B.

- Hedman, E. I. Solomon, C. J. Cramer, W. B. Tolman, *J. Am. Chem. Soc.* **2004**, *126*, 16896–16911; d) W. H. Monillas, G. P. A. Yap, L. A. MacAdams, K. H. Theopold, *J. Am. Chem. Soc.* **2007**, *129*, 8090–8091; e) A. R. Sadique, W. W. Brennessel, P. L. Holland, *Inorg. Chem.* **2008**, *47*, 784–786; f) T. R. Dugan, P. L. Holland, *J. Organomet. Chem.* **2009**, *694*, 2825–2830; g) D. J. Mindiola, *Angew. Chem.* **2009**, *121*, 6314–6316; *Angew. Chem. Int. Ed.* **2009**, *48*, 6198–6200; h) Y.-C. Tsai, *Coord. Chem. Rev.* **2012**, *256*, 722–758; i) S. Yao, M. Driess, *Acc. Chem. Res.* **2012**, *45*, 276–287.
- [7] a) S. Pfirrmann, C. Limberg, B. Ziemer, *Dalton Trans.* **2008**, 6689–6691; b) S. Pfirrmann, C. Limberg, C. Herwig, *Angew. Chem.* **2009**, *121*, 3407–3411; *Angew. Chem. Int. Ed.* **2009**, *48*, 3357–3361.
- [8] S. Pfirrmann, S. Yao, B. Ziemer, R. Stösser, M. Driess, C. Limberg, *Organometallics* **2009**, *28*, 6855–6860.
- [9] A further example was reported only recently; see: S. J. Tereniak, E. E. Marlier, C. C. Lu, *Dalton Trans.* **2012**, *41*, 7862–7865.
- [10] S. O. N. Lill, P. E. M. Siegbahn, *Biochemistry* **2009**, *48*, 1056–1066.
- [11] S. Pfirrmann, C. Limberg, C. Herwig, C. Knispel, B. Braun, E. Bill, R. Stösser, *J. Am. Chem. Soc.* **2010**, *132*, 13684–13691.
- [12] a) D. F.-J. Piesik, S. Range, S. Harder, *Organometallics* **2008**, *27*, 6178–6187; b) J. Spielmann, D. F.-J. Piesik, S. Harder, *Chem. Eur. J.* **2010**, *16*, 8307–8318; c) S. Harder, J. Spielmann, J. Intemann, H. Bandmann, *Angew. Chem.* **2011**, *123*, 4242–4246; *Angew. Chem. Int. Ed.* **2011**, *50*, 4156–4160.
- [13] M. Al-Anber, B. Walfort, S. Vatsadze, H. Lang, *Inorg. Chem. Commun.* **2004**, *7*, 799–802.
- [14] R. Knorr, H. Hauer, A. Weiss, H. Polzer, F. Ruf, P. Löw, P. Dvortsák, P. Böhrer, *Inorg. Chem.* **2007**, *46*, 8379–8390.
- [15] A. Pardo, A. L. De Lacey, V. M. Fernández, H.-J. Fan, Y. Fan, M. B. Hall, *J. Biol. Inorg. Chem.* **2006**, *11*, 286–306.
- [16] a) M. Jiménez Tenorio, M. C. Puerta, P. Valerga, *J. Chem. Soc. Dalton Trans.* **1996**, 1305–1308; b) M. G. Crestani, M. Muñoz-Hernández, A. Arévalo, A. Acosta-Ramírez, J. J. García, *J. Am. Chem. Soc.* **2005**, *127*, 18066–18073.
- [17] J. Breitenfeld, R. Scopelliti, X. Hu, *Organometallics* **2012**, *31*, 2128–2136.
- [18] M. J. Frisch, G. W. Trucks, H. B. Schlegel, G. E. Scuseria, M. A. Robb, J. R. Cheeseman, G. Scalmani, V. Barone, B. Mennucci, G. A. Petersson, H. Nakatsuji, M. Caricato, X. Li, H. P. Hratchian, A. F. Izmaylov, J. Bloino, G. Zheng, J. L. Sonnenberg, M. Hada, M. Ehara, K. Toyota, R. Fukuda, J. Hasegawa, M. Ishida, T. Nakajima, Y. Honda, O. Kitao, H. Nakai, T. Vreven, J. A. Montgomery, Jr., J. E. Peralta, F. Ogliaro, M. Bearpark, J. J. Heyd, E. Brothers, K. N. Kudin, V. N. Staroverov, R. Kobayashi, J. Normand, K. Raghavachari, A. Rendell, J. C. Burant, S. S. Iyengar, J. Tomasi, M. Cossi, N. Rega, J. M. Millam, M. Klene, J. E. Knox, J. B. Cross, V. Bakken, C. Adamo, J. Jaramillo, R. Gomperts, R. E. Stratmann, O. Yazyev, A. J. Austin, R. Cammi, C. Pomelli, J. W. Ochterski, R. L. Martin, K. Morokuma, V. G. Zakrzewski, G. A. Voth, P. Salvador, J. J. Dannenberg, S. Dapprich, A. D. Daniels, Ö. Farkas, J. B. Foresman, J. V. Ortiz, J. Cioslowski, and D. J. Fox, *Gaussian 09*, Revision C.01; Gaussian, Inc., Wallingford CT, **2010**.
- [19] a) G. Bai, P. Wei, D. W. Stephan, *Organometallics* **2005**, *24*, 5901–5908; b) E. Kogut, H. L. Wiencko, L. Zhang, D. E. Cordeau, T. H. Warren, *J. Am. Chem. Soc.* **2005**, *127*, 11248–11249; c) V. V. Saraev, P. B. Kraikivskii, I. Svoboda, S. Kuzakov, R. F. Jordan, *J. Phys. Chem. A* **2008**, *112*, 12449–12455.
- [20] a) K. Frazee, A. D. Wilson, A. M. Appel, M. R. DuBois, D. L. DuBois, *Organometallics* **2007**, *26*, 3918–3924; b) M. L. Helm, M. P. Stewart, R. M. Bullock, M. R. DuBois, D. L. DuBois, *Science* **2011**, *333*, 863–866; c) D. L. DuBois, R. M. Bullock, *Eur. J. Inorg. Chem.* **2011**, 1017–1027; d) S. Raugei, S. Chen, M.-H. Ho, B. Ginovska-Pangovska, R. J. Rousseau, M. Dupuis, D. L. DuBois, R. M. Bullock, *Chem. Eur. J.* **2012**, *18*, 6493–6506.
- [21] a) M. Ito, T. Matsumoto, K. Tatsumi, *Inorg. Chem.* **2009**, *48*, 2215–2223; b) T. Li, J. J. García, W. W. Brennessel, W. D. Jones, *Organometallics* **2010**, *29*, 2430–2445; c) A. Velian, S. Lin, A. J. M. Miller, M. W. Day, T. Agapie, *J. Am. Chem. Soc.* **2010**, *132*, 6296–6297.
- [22] a) X. Zhao, I. P. Georgakaki, M. L. Miller, J. C. Yarbrough, M. Y. Darensbourg, *J. Am. Chem. Soc.* **2001**, *123*, 9710–9711; b) F. Gloaguen, J. D. Lawrence, T. B. Rauchfuss, *J. Am. Chem. Soc.* **2001**, *123*, 9476–9477; c) F. Gloaguen, J. D. Lawrence, T. B. Rauchfuss, M. Bénard, M.-M. Rohme, *Inorg. Chem.* **2002**, *41*, 6573–6582; d) F. Gloaguen, T. B. Rauchfuss, *Chem. Soc. Rev.* **2009**, *38*, 100–108.
- [23] a) D. F. Evans, *J. Chem. Soc.* **1959**, 2003–2005; b) E. M. Schubert, *J. Chem. Educ.* **1992**, *69*, 62; c) T. Ayers, R. Turk, C. Lane, J. Goins, D. Jameson, S. Slattery, *Inorg. Chim. Acta* **2004**, *357*, 202–206.
- [24] G. A. Bain, J. F. Berry, *J. Chem. Educ.* **2008**, *85*, 532–536.
- [25] G. Sheldrick, *Acta Crystallogr. Sect. A* **2008**, *64*, 112–122.

Received: September 8, 2012
Published online: ■ ■ ■, 0000

Ni-H in the claw: An investigation of the chemistry of nickel hydride within a ligand framework that is composed of two β -diketiminato binding sites has led to the observation of remarkable reactivities and rare structural features, including a mixed-valent dinickel-hydride core (see figure) and a thio-late-bridged Ni^INi^I complex.

**Mixed-Valent Compounds**

*H. Gehring, R. Metzinger, C. Herwig,
J. Intemann, S. Harder,
C. Limberg**



**Hydride Reactivity of Ni^I-X-Ni^{II}
Entities: Mixed-Valent Hydrido
Complexes and Reversible Metal
Reduction**

